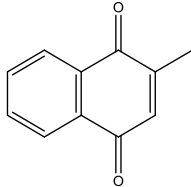
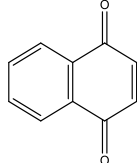
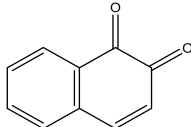
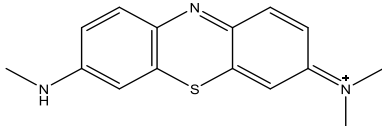
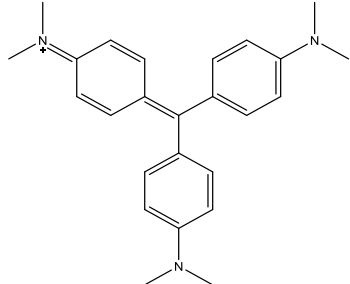
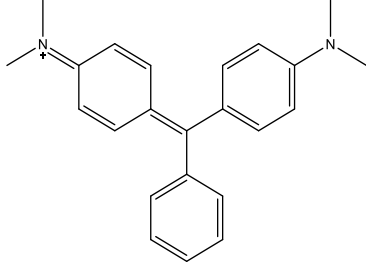
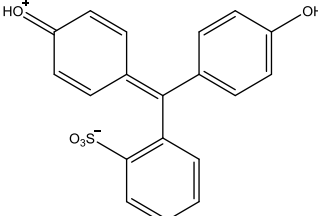
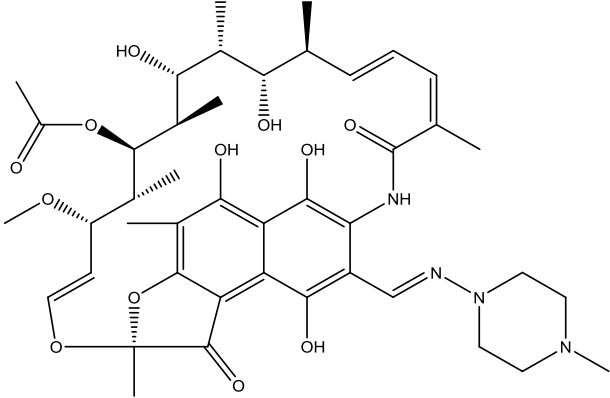
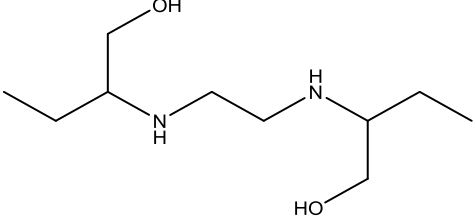
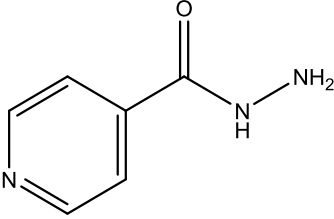
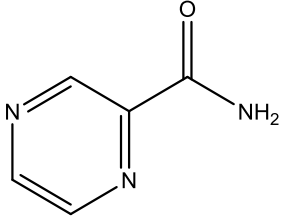
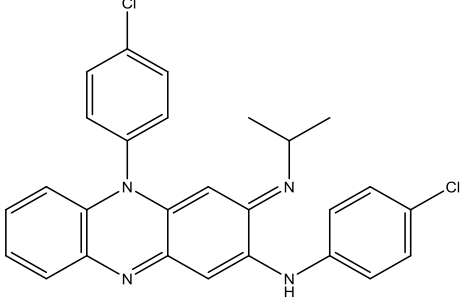
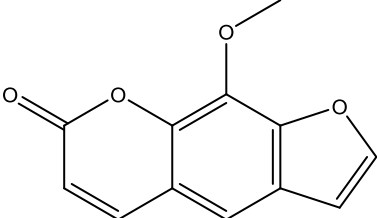
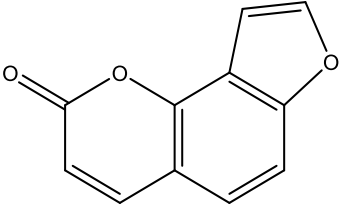


Supporting Information

Table S1. Chemical structures of the 20 compounds studied.

Family	Substrates	Structures
Quinones	Menadione (172.18 Da)	
	1,4-naphthoquinone (158.15 Da)	
	1,2-naphthoquinone (158.15 Da)	
Triphenyls	Azure B (270.38 Da)	
	Crystal violet (372.53 Da)	
	Malachite green (329.46 Da)	
	Phenol red (354.38 Da)	

First-line antimycobacterials	Rifampicin (822.94 Da)	
	Ethambutol (204.31 Da)	
	Isoniazid (137.14 Da)	
	Pyrazinamide (123.11 Da)	
	Clofazimine (473.40 Da)	
Furanocoumarins and aminocoumarins	Methoxsalen (216.19 Da)	
	Angelicin (186.17 Da)	

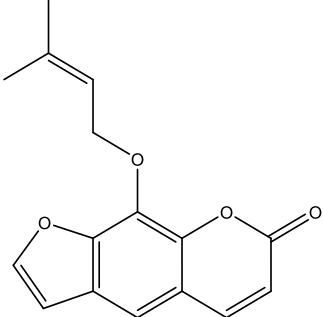
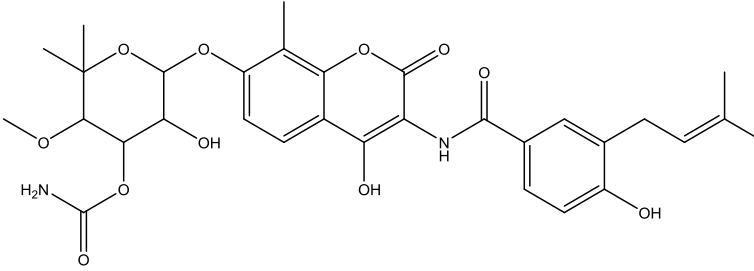
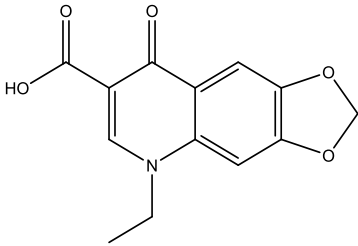
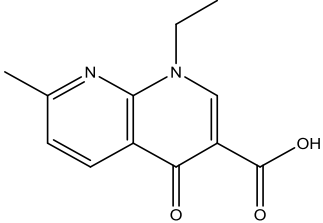
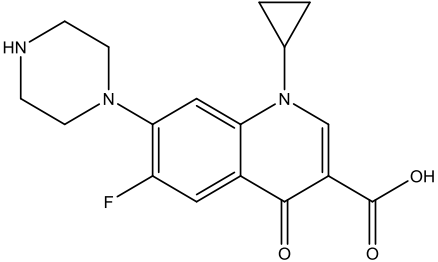
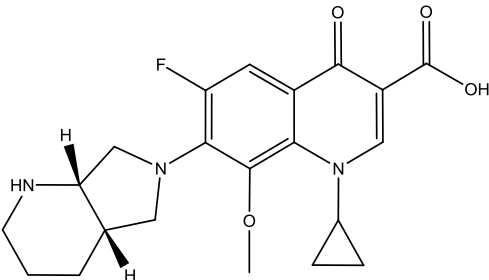
	<p>Imperatorin (270.28 Da)</p>	
	<p>Novobiocin (612.12 Da)</p>	
<p>Quinolones and fluoroquinolones</p>	<p>Oxolinic acid (261.23 Da)</p>	
	<p>Nalidixic acid (232.24 Da)</p>	
	<p>Ciprofloxacin (331.35 Da)</p>	
	<p>Moxifloxacin (401.43 Da)</p>	

Table S2. Comparison of specific activities of F₄₂₀H₂ reoxidation and substrate reduction for selected compounds in the presence of the FDOR-A1 enzyme MSMEG_2027. F₄₂₀H₂ reoxidation was measured by absorbance at 420 nm, whereas substrate reduction was measured by the size of elution peaks on HPLC. Specific activities are expressed in nmol min⁻¹ μmol⁻¹ enzyme.

Substrate	Rate of cofactor oxidation	Rate of substrate reduction
1,2-naphthoquinone	85200 ± 3100	108000 ± 6100
Methoxsalen	1230 ± 20	1700 ± 250
Imperatorin	1710 ± 30	1400 ± 210
Malachite green	420 ± 10	900 ± 400
Rifampicin	28.2 ± 2.0	21.8 ± 9.1

Figure S1. F₄₂₀-dependent survival of *M. smegmatis* following challenge with rifampicin at 5 × MIC of the wild-type strain. The survival of three strains, the wild-type, *fgd* mutant, and *fbiC* mutant, was determined by colony forming units Error bars represent standard deviations from three biological replicates. *p*-values were calculated by comparing CFU counts between wild-type and mutant strains, where * = *p* < 0.05, ** = *p* < 0.01, *** = *p* < 0.001, and ns = not significant.

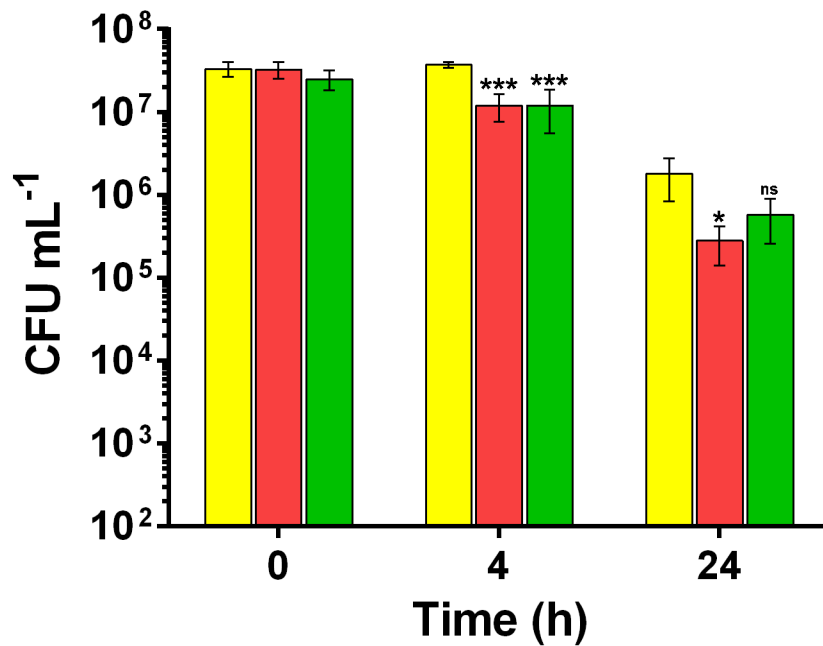


Figure S2. SDS-PAGE gels showing recombinant expression and purification of six F₄₂₀H₂-dependent FDORs and Fgd from *Mycobacterium smegmatis*. From left to right, the gels shown are MSMEG_5998 (A1), MSMEG_2027 (A1), MSMEG_6325 (A3), MSMEG_0048 (B1), MSMEG_3380 (B1), MSMEG_5170 (B1), and Fgd. Bands corresponding to the dimeric and tetrameric forms of the FDORs are visible. Legend: M = standard protein marker, WC = whole-cell lysate, S = soluble fraction, FT = flow-through, E1 to E8 = eluted protein fractions 1 to 8.

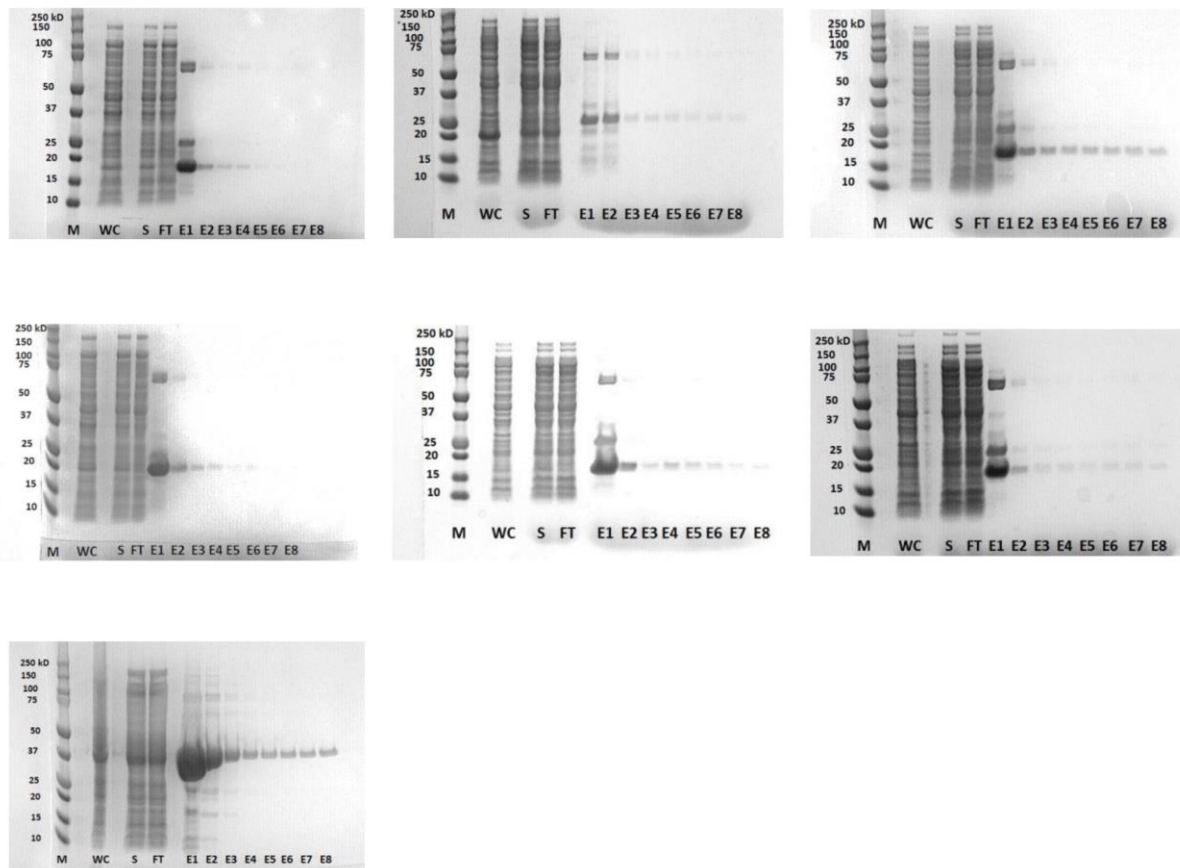


Figure S3. Rate of F_{420H_2} -dependent, enzyme-independent substrate reduction. The five substrates with significant reduction rates are shown.

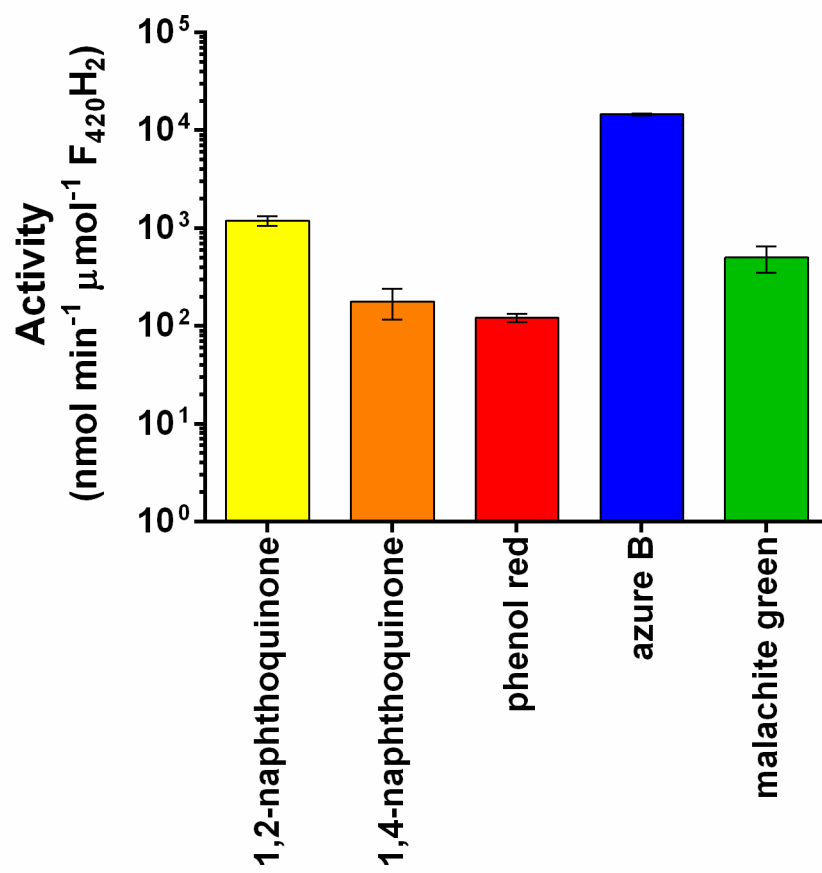
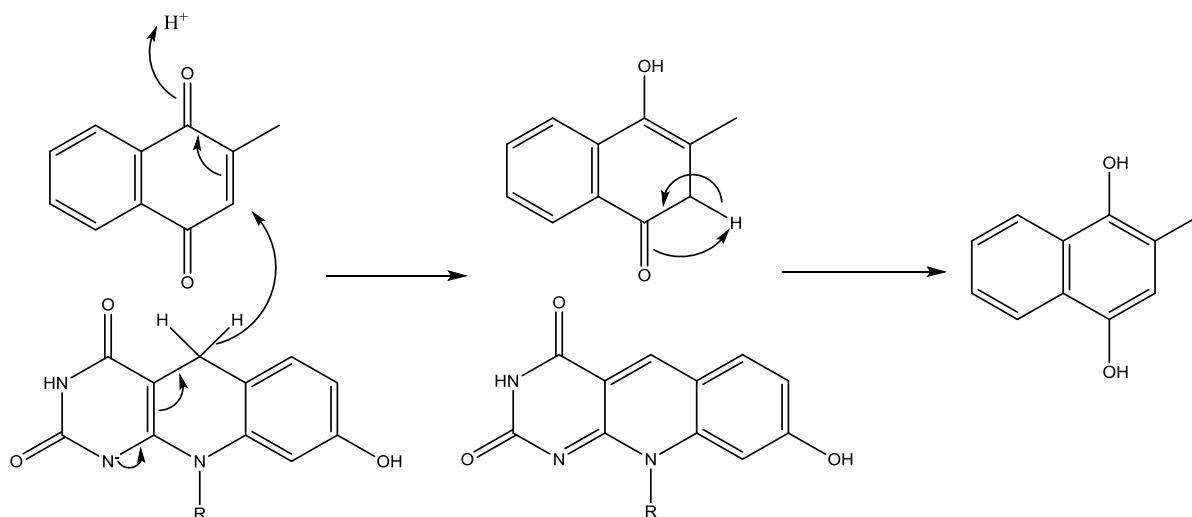
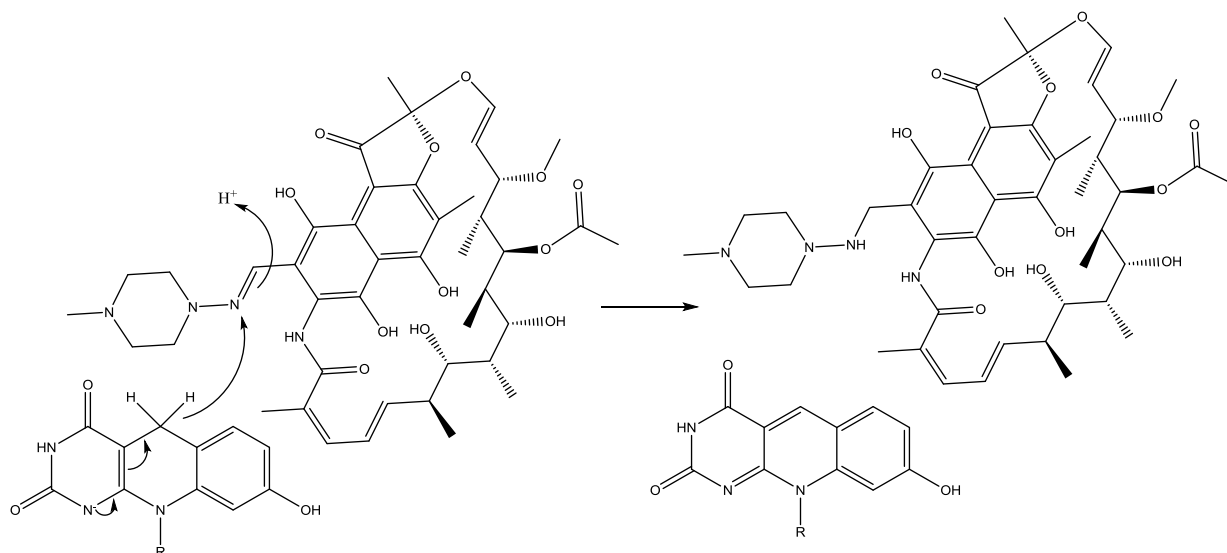


Figure S4. Proposed reaction mechanisms for the F₄₂₀H₂-dependent reduction of representative compounds from each compound class. The mechanisms for menadione (quinone analog), rifampicin, and clofazimine are shown here. The mechanisms for methoxsalen (furanocoumarin), malachite green (arylmethane dye) are shown in **Figure 3**.

Menadione:



Rifampicin:



Clofazimine:

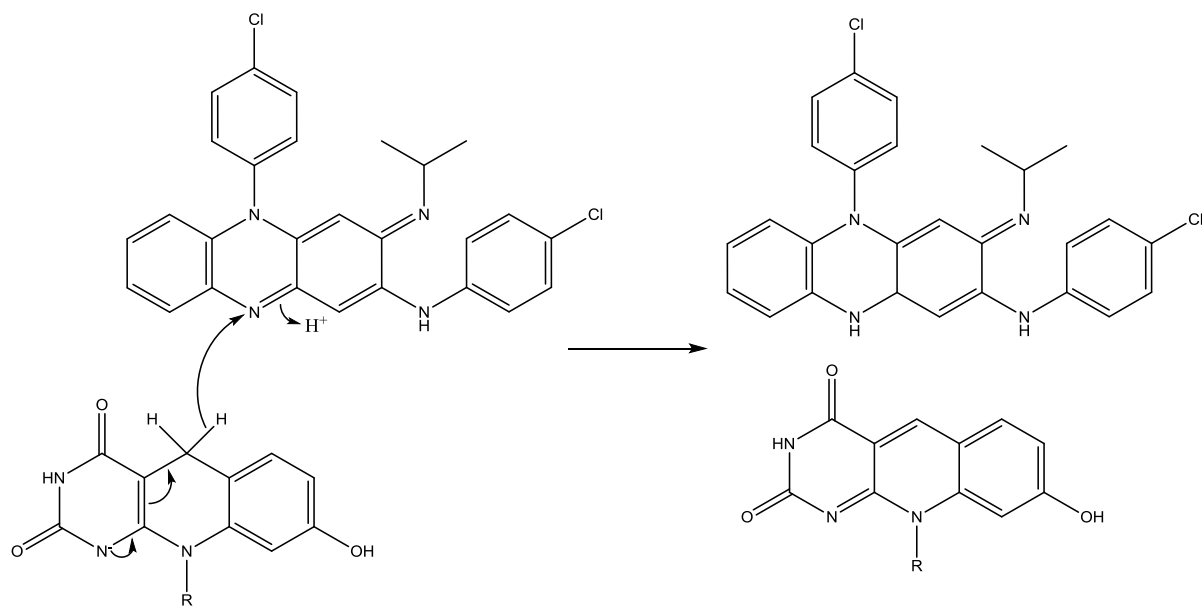


Figure S5. Correlation between FDOR activities and MIC ratios. The y-axis shows the maximum specific activity of the FDORs for the 20 compounds tested. The x-axis shows the ratio of the MIC of the wild-type and *fbiC:kan* mutant strains of *M. smegmatis* for the 20 compounds.

